JACC: CARDIOVASCULAR IMAGING
VOL. 9, NO. 1, 2016

ISSN 1936-878X/$36.00
PUBLISHED BY ELSEVIER
http://dx.doi.org/10.1016/j.jcmg.2015.11.008

Automatic Measurement of the Myocardial Interstitium

Synthetic Extracellular Volume Quantification Without Hematocrit Sampling

Thomas A. Treibel, MBBS,*† Marianna Fontana, MD,*† Viviana Maestrini, MD,*‡ Silvia Castelletti, MD,*† Stefania Rosmini, MD,*† Joanne Simpson, MBBS,* Arthur Nasis, MD,* Anish N. Bhuva, MBBS,*† Heerajnarain Bulluck, MBBS,*† Amna Abdel-Gadir, MBBS,*† Steven K. White, MB, ChB,*† Charlotte Manisty, PhD,*† Bruce S. Spottiswoode, PhD,§ Timothy C. Wong, MD,‖ Stefan K. Piechnik, PhD, MScEE,¶ Peter Kellman, PhD,# Matthew D. Robson, PhD,¶ Erik B. Schelbert, MD, MS,‖ James C. Moon, MD*†

ABSTRACT

OBJECTIVES The authors sought to generate a synthetic extracellular volume fraction (ECV) from the relationship between hematocrit and longitudinal relaxation rate of blood.

BACKGROUND ECV quantification by cardiac magnetic resonance (CMR) measures diagnostically and prognostically relevant changes in the extracellular space. Current methodologies require blood hematocrit (Hct) measurement—a complication to easy clinical application. We hypothesized that the relationship between Hct and longitudinal relaxation rate of blood ($R1 = 1/T1_{blood}$) could be calibrated and used to generate a synthetic ECV without Hct that was valid, user-friendly, and prognostic.

METHODS Proof-of-concept: 427 subjects with a wide range of health and disease were divided into derivation ($n = 214$) and validation ($n = 213$) cohorts. Histology cohort: 18 patients with severe aortic stenosis with histology obtained during valve replacement. Outcome cohort: For comparison with external outcome data, we applied synthetic ECV to 1,172 consecutive patients (median follow-up 1.7 years; 74 deaths). All underwent CMR scanning at 1.5-T with ECV calculation from pre- and post-contrast T1 (blood and myocardium) and venous Hct.

RESULTS Proof-of-concept: In the derivation cohort, native $R1_{blood}$ and Hct showed a linear relationship ($R^2 = 0.51$; $p < 0.001$), which was used to create synthetic Hct and ECV. Synthetic ECV correlated well with conventional ECV ($R^2 = 0.97$; $p < 0.001$) without bias. These results were maintained in the validation cohort. Histology cohort: Synthetic and conventional ECV both correlated well with collagen volume fraction measured from histology ($R^2 = 0.61$ and 0.69, both $p < 0.001$) with no statistical difference ($p = 0.70$). Outcome cohort: Synthetic ECV related to all-cause mortality (hazard ratio 1.90; 95% confidence interval 1.55 to 2.31; for every 5% increase in ECV). Finally, we engineered a synthetic ECV tool, generating automatic ECV maps during image acquisition.

CONCLUSIONS Synthetic ECV provides validated noninvasive quantification of the myocardial extracellular space without blood sampling and is associated with cardiovascular outcomes. (J Am Coll Cardiol Img 2016;9:54–63) © 2016 by the American College of Cardiology Foundation.

From the *Barts Heart Centre, St Bartholomew's Hospital, London, United Kingdom; †Institute of Cardiovascular Science, University College London, London, United Kingdom; ‡Department of Cardiovascular, Respiratory, Nephrology, Anesthesiology & Geriatric Sciences, Sapienza University, Rome, Italy; §Siemens Healthcare, Chicago, Illinois; ‖UPMC Heart and Vascular Institute, University of Pittsburgh, Pittsburgh, Pennsylvania; ¶Division of Cardiovascular Medicine, Radcliffe Department of Medicine, University of Oxford, John Radcliffe Hospital, Oxford, United Kingdom; and the #National Heart, Lung, and Blood Institute, National Institute for Health, Bethesda, Maryland. Drs. Treibel and Fontana are supported by doctoral research fellowships by the U.K. National Institute of Health Research and British Heart Foundation, respectively. Dr. Spottiswoode is an employee of Siemens Medical Solutions USA, Inc. Dr. Wong was supported by a grant from the Agency for Healthcare Research and Quality. Drs. Piechnik and Robson are supported by the NIHR Oxford Biomedical Research Centre, Oxford University Hospitals Trust, University of Oxford. Dr. Schelbert was supported by grants from The Pittsburgh Foundation, and

In health and disease, cardiac function is governed by an intricate interplay between myocardial cellular and interstitial components (1). Changes in the extracellular matrix (ECM) occur in adverse remodeling, e.g. diffuse fibrosis (2-4). Cardiac magnetic resonance (CMR) now permits measurement of this by using T1 mapping to quantify the extracellular volume fraction (ECV) (5,6). T1 mapping measures the longitudinal relaxation time, which is altered by myocardial fibrosis, edema, iron overload, and infiltrative diseases like amyloidosis (7,8). After administration of a gadolinium-based extracellular contrast agent, T1 is shortened. The ECV is derived from the ratio of changes in signal in myocardium and blood pre- and post-contrast and involves correction for the blood hematocrit. Early data suggests that ECV predicts mortality and major adverse cardiac events independently and as well as left ventricular ejection fraction excluding hypertrophic cardiomyopathy, amyloidosis, or congenital heart disease (9,10). Hematocrit (Hct) measurement is needed, which is cumbersome, introduces variability, and delays workflow, impeding adoption of the method (11-13).

The longitudinal relaxivity (R1 = 1/T1) of blood has been studied since the 1980s and was found to be in a linear relationship with blood Hct. It is determined by the water fractions of plasma and the erythrocyte cytoplasm, which undergo fast water exchange (7,14-20).

We hypothesize that this relationship could be used to estimate a synthetic Hct, permitting immediate synthetic ECV calculation without blood sampling. We formed a network of collaboration with existing key patient cohorts to investigate whether synthetic ECV: 1) was valid compared to conventional ECV; 2) correlated with the gold standard collagen volume fraction (CVF); 3) predicted outcome and 4) could be automated for in-line point-of-care use.

SEE PAGE 64

METHODS

PATIENT POPULATIONS. Research was carried out at 2 centers (**Table 1**): University College London Hospital NHS Trust, United Kingdom (proof-of-concept and histology cohorts); and UPMC CMR Center, Pittsburgh, Pennsylvania (outcome cohort). Study approvals were granted by local ethics committees, and conformed to the principles of the Helsinki Declaration. ECV data of 2 previously published cohorts was used to validate the synthetic ECV methodology (histology and outcome cohorts).

Proof-of-concept of synthetic ECV: cohorts 1 (derivation) and 2 (validation). A total of n = 427 subjects gave written informed consent and were scanned between January 2012 and October 2014. They were then randomly split into derivation and validation subgroups (**Table 2**) with equal health and disease representation.

Normal healthy subjects (n = 66, median age 45 ± 14 years [range 24 to 74 years], 59% male), with no history or symptoms of cardiovascular disease or diabetes: All had normal blood pressure (defined as <140/90 mm Hg), 12-lead electrocardiogram, and clinical CMR results.

Hypertrophic cardiomyopathy patients (n = 68, median age 52 ± 14 years [range 23 to 77 years], 81% male): All met previously described diagnostic criteria (21). Hypertrophy was 81% asymmetrical, 9% concentric, and 10% apical predominant.

Severe aortic stenosis (AS) patients (n = 123, median age 70 ± 10 years [range 34 to 84 years], 55% male): All had undergone clinical evaluation and echocardiography for diagnosis of severe AS and were listed for surgical valve replacement.

Cardiac amyloidosis patients (n = 74, median age 72 ± 11 years [range 38 to 85 years], 82% male): Cardiac amyloid was only transthyretin amyloid (ATTR). This was defined by either a myocardial biopsy, or positive bone scintigraphy. Patients underwent sequencing of exons 2, 3, and 4 of the *TTR* gene. Consensus criteria for definite cardiac involvement are pending, but not published: definite cardiac transthyretin amyloid was defined as previously described (22,23).

Patients post-anthracycline chemotherapy for histologically proven breast carcinoma at a median follow-up of 6.4 years (n = 96, median age 54 years [range 28 to 71 years], 100% female, 100% Caucasian), with no previous chemo- or radiotherapy or any pre-existing cardiovascular disease or drug history.

ABBREVIATIONS AND ACRONYMS

AS = aortic stenosis
CMR = cardiac magnetic resonance
CVF = collagen volume fraction
ECM = extracellular matrix
ECV = extracellular volume fraction
Hct = hematocrit
HHF = hospitalization for heart failure
MOCO = motion correction
MOLLI = MOdified Look-Locker Inversion recovery
ShMOLLI = Shortened MOdified Look-Locker Inversion recovery

the American Heart Association Scientist Development fund; he has accepted contrast material from Bracco Diagnostics for research purposes beyond the scope of this work. Prof. Moon is directly and indirectly supported by the University College London Hospitals NIHR Biomedical Research Centre and Biomedical Research Unit at Barts Hospital, respectively. All other authors have reported that they have no relationships relevant to the contents of this paper to disclose.

Manuscript received September 28, 2015; revised manuscript received November 30, 2015, accepted November 30, 2015.

JACC: CARDIOVASCULAR IMAGING, VOL. 9, NO. 1, 2016
JANUARY 2016:54–63

TABLE 1 Overview of Study Cohorts

	Subjects	Location	Characteristics
Proof-of-concept	n = 427	London, UK	Health and disease, split into derivation and validation cohorts (Table 2).
Histology	n = 18	London, UK	Severe aortic stenosis patients undergoing aortic valve replacement (with intraoperative myocardial biopsy)
Outcome	n = 1,172	Pittsburgh, PA	Clinical cohort referred for CMR (Online Table S1)

CMR = cardiovascular magnetic resonance.

HISTOLOGICAL VALIDATION OF SYNTHETIC ECV: HISTOLOGY COHORT. Consenting (same center) severe AS patients (n = 18, median age 71 ± 10 years [range 47 to 84 years], 78% male) were scanned between May 2011 and February 2012. All had undergone clinical evaluation and echocardiography for diagnosis before surgical aortic valve replacement, and intraoperative biopsies were obtained for histological measurement of CVF as previously described (24).

TABLE 2 Patient Characteristics for Derivation and Validation of Synthetic Hct

	Derivation (n = 214)	Validation (n = 213)	p Value
Male	107	104	0.8
Age, yrs	60 ± 15	60 ± 15	0.6
BSA, m^2	1.87 ± 0.23	1.87 ± 0.23	0.8
Healthy volunteer	33	33	
Aortic stenosis	62	61	
Cardiac amyloidosis	37	37	
Hypertrophic cardiomyopathy	34	34	
Anthracycline	48	48	
Cardiac			
EDVi, ml/m^2	71 ± 21	70 ± 20	0.9
ESVi, ml/m^2	25 ± 14	24 ± 13	0.5
LV mass index, g/m^2	90 ± 35	92 ± 35	0.5
Stroke volume index, ml/m^2	47 ± 12	47 ± 13	0.7
LVEF, %	66 ± 12	67 ± 12	0.7
LAAi, cm^2/m^2	14 ± 3	14 ± 5	0.5
Clinical			
Hematocrit	0.40 ± 0.04	0.40 ± 0.04	0.4
Creatinine, micromol/l	79 ± 24	78 ± 21	0.9
eGFR, mls/min/1.73 m^2	80 ± 23	78 ± 22	0.4
SBP, mm Hg	110 ± 44	108 ± 49	0.7
DBP, mm Hg	65 ± 28	62 ± 31	0.5
T1 mapping			
ShMOLLI ECV, %	33 ± 10	33 ± 11	0.9
MOLLI ECV, %	33 ± 11	33 ± 11	0.8

Values are n or mean ± SD.

BSA = body surface area; DBP = diastolic blood pressure; ECV = extracellular volume fraction; EDVi = indexed end-diastolic volume; ESVi = indexed end-systolic volume; eGFR = estimated glomerular filtration rate; Hct = hematocrit; LAAi = indexed left atrial area; LVEF = left ventricular ejection fraction; MOLLI = MOdified Look-Locker Inversion recovery; ShMOLLI = Shortened MOdified Look-Locker Inversion recovery; SBP = systolic blood pressure.

CORRELATION OF SYNTHETIC ECV WITH OUTCOME: OUTCOME COHORT. For external validation of synthetic ECV and comparison with outcome data, we applied the method to a large ECV outcome cohort (25): 1,765 consecutive adult patients referred for clinical CMR at UPMC CMR Center, Pittsburgh, Pennsylvania (enrolled December 2009 to May 2013; follow-up until July 2013). Inclusion criteria were written informed consent and completion of contrast CMR. Exclusion criteria were cardiac amyloidosis (n = 27), hypertrophic cardiomyopathy (n = 133), stress-induced cardiomyopathy (n = 10), adult congenital heart disease (n = 195), inadequate image quality (n = 4), and missing follow-up (n = 224). Patients with myocardial infarction were included to maximize generalizability (ECV measured in remote noninfarcted myocardium). The final cohort included 1,172 patients (Table 3).

AUTOMATED INLINE ECV: SYNTHETIC ECV MAPS "ON-THE-FLY". An investigational prototype ECV tool, previously developed by Kellman et al. (26,27), was adapted to measure $T1_{blood}$, calculate synthetic Hct, and generate inline synthetic ECV maps as DICOM images on the CMR scanner; fully automated using coregistration and blood pool segmentation.

CMR SCANNING. All subjects underwent CMR at 1.5-T (Magnetom Avanto, Espree, and Aera, Siemens Medical Solutions, Malvern, Pennsylvania) with 32-channel cardiac coil arrays. Exclusion criteria were uncontrolled arrhythmia, impaired renal function (estimated glomerular filtration rate <30 ml/min), or contraindications to magnetic resonance imaging (e.g., implanted devices). Specific details are listed in the individual cohort descriptions. All patients underwent standard clinical scan with late gadolinium imaging (28) with T1 mapping before and after bolus gadolinium contrast: for the proof-of-concept and histology cohorts, 0.1 mmol/kg of gadoterate meglumine, (gadolinium-DOTA, marketed as Dotarem, Guerbet S.A., Paris, France); for the outcome cohort, 0.2 mmol/kg intravenous gadoteridol bolus (ProHance, Bracco Diagnostics, Princeton, New Jersey). Post-contrast imaging was performed at 15 to 20 min apart from amyloid patients, where we acquired equilibrium-contrast T1 maps (24,29). The T1 mapping sequences used were balanced steady-state free precession-based MOdified Look-Locker Inversion Recovery (MOLLI) (11) variants (investigational prototypes): in the proof-of-concept cohort, both a Shortened MOdified Look-Locker Inversion recovery (ShMOLLI) sequence and a MOLLI variant with motion correction were used (30,31). The histological validation was performed with ShMOLLI, whereas the outcome

TABLE 3 Clinical Characteristics of the Outcome Cohort

Demographics	N = 1,172
Age, yrs	56 (43-66)
Female	484 (48)
White race	1033 (88)
Black race	112 (10)
Comorbidity	
Diabetes	239 (20)
Hypertension	585 (50)
Dyslipidemia	448 (38)
Atrial fibrillation or flutter	121 (10)
Prior coronary revascularization	217 (19)
Body mass index, kg/m^2	28 (25-33)
Laboratory and CMR characteristics	
Creatinine, mg/dl	0.9 (0.8-1.1)
Glomerular filtration rate, ml/min/1.73 m^2	89 (70-94)
Ejection fraction, %	57 (45-64)
Left ventricular mass index, g/m^2	57 (46-71)
End diastolic volume index, ml/m^2	82 (67-101)
End systolic volume index, ml/m^2	34 (25-51)
Myocardial infarction	238 (20)
Nonischemic fibrosis evident on LGE images	236 (20)
Extracellular volume fraction, %	28 (26-31)

Values are median (interquartile range) or n (%).
CMR = cardiac magnetic resonance; LGE = late gadolinium enhancement.

cohort was performed with a MOLLI with motion correction (for sequence parameters see Supplementary material).

T1 ANALYSIS AND ECV QUANTIFICATION. A region of interest was drawn in myocardium (in the septum on a short-axis slice) and blood (same slice) on the pre-contrast images and transposed to the post-contrast images. All analysis was performed blinded. We quantified ECM expansion with ECV defined as (8):

$$\mathrm{ECV} = (1 - \mathrm{hematocrit}) \cdot [\Delta \mathrm{R1}_{\mathrm{myocardium}}] / [\Delta \mathrm{R1}_{\mathrm{bloodpool}}]$$

$$(\text{where, } \Delta R1_{myocardium} = R1^{post-contrast}_{myocardium} - R1^{pre-contrast}_{myocardium}$$

$$\Delta R1_{blood} = R1^{post-contrast}_{blood} - R1^{pre-contrast}_{blood}$$
$$\mathrm{R1} = 1/\mathrm{T1})$$

LABORATORY HCT VARIABILITY. Whole blood for venous Hct was drawn in all subjects by venipuncture and analyzed as routine clinical samples using a Sysmex XE-2100 hematology analyzer (Sysmex, Kobe, Japan) (32). Repeat sampling variability was tested in 44 patients who underwent 2 samples a median of 4 h apart.

SYNTHETIC HCT DERIVATION. The longitudinal relaxivity (R1 = 1/T1) of blood has a linear relationship with blood Hct, and is determined by the relaxivity of the water fractions of plasma ($\mathrm{R1_P}$) and the erythrocyte cytoplasm ($\mathrm{R1_{RBC}}$) (19):

$$\mathrm{R1_{Blood}} = \mathrm{R1_P} \cdot (1 - \mathrm{Hct}) + \mathrm{R1_{RBC}} \cdot \mathrm{Hct}$$

$$\text{Rearranging gives: } \mathrm{Hct} = -\mathrm{R1_P}/(\mathrm{R1_{RBC}} - \mathrm{R1_P}) + \mathrm{R1_{Blood}} \cdot [1/(\mathrm{R1_{RBC}} - \mathrm{R1_P})]$$

$$\text{Simplified as: } \mathrm{Hct} = \mathrm{Constant\#1} + (\mathrm{Constant\#2} \cdot \mathrm{R1_{blood}})$$

Therefore, synthetic Hct was derived from the linear relationship between Hct and $\mathrm{R1_{blood}}$, in turn used to estimate a synthetic ECV and was then compared with the conventional ECV.

HISTOLOGICAL ANALYSIS OF CVF. Histological quantification of the extracellular space was performed by measuring the CVF as previously described (24). In summary, an intraoperative deep myocardial biopsy (Tru-Cut-type biopsy) was taken from the basal left ventricular septum, stained with Picrosirius red, photographed at high-power magnification (200 μm), and CVF (%) automatically quantified over an average of 12 high-power fields with a purpose-written macro in ImageJ version 1.43, 2009 (National Institutes of Health, Bethesda, Maryland). All samples were analyzed blinded to other findings.

STATISTICAL ANALYSIS. Analyses were performed using SAS version 9.3 (Cary, North Carolina) and SPSS version 22 (Chicago, Illinois). All data are presented as mean ± SD for individuals or measurements as indicated. Differences were assessed using unpaired Student *t* tests to simulate independent group comparisons. Statistical tests were 2-sided. Significance was quoted when probability was <0.05 divided by the number of simultaneous comparisons in the relevant analysis (Bonferroni correction). Agreement between conventional and synthetic ECV was analyzed using the Bland-Altman method. The significance of the difference between 2 correlation coefficients was tested using the Fisher r-to-z transformation. Survival analyses examined: time to the first hospitalization for heart failure (HHF) after CMR, time to death, and time to either HHF or death. First HHF included any HHF event after CMR, and required physician documentation of: 1) symptoms and physical signs consistent with HF; 2) supporting clinical findings; or 3) therapy for HF. Vital status was ascertained by Social Security Death Index queries and medical record review (confirmed by 2 blinded investigators, E.B.S. and T.C.W.). Mortality was right censored for the first HHF after CMR analysis. The log-rank test with ECV (categorized arbitrarily in 5% increments) and Cox regression (ECV expressed as a continuous variable) examined associations between ECV and outcomes (more in the Online Appendix).

JACC: CARDIOVASCULAR IMAGING, VOL. 9, NO. 1, 2016
JANUARY 2016:54–63

RESULTS

PROOF-OF-CONCEPT: DERIVATION AND VALIDATION COHORTS. The proof-of-concept cohort was divided randomly into a derivation (n = 214) and a validation (n = 213) cohort (**Table 2**). In the derivation cohort, there was a broad range of Hct (40.3 ± 3.7%; range 32% to 51%) and native $T1_{blood}$ (ShMOLLI $T1_{blood}$ 1,549 ± 80 ms; range 1,261 to 1,823 ms; MOLLI $T1_{blood}$ 1,649 ± 83 ms; range 1,441 to 1,898 ms). The regression line between hematocrit and $R1_{blood}$ ($1/T1_{blood}$) was linear with $R^2 = 0.51$, $p < 0.001$; and 0.45, $p < 0.001$; for MOLLI and ShMOLLI, respectively (**Figure 1**). The regression equations were:

$$\text{Synthetic Hct}_{\text{MOLLI}} = (866.0 \cdot [1/T1_{blood}]) - 0.1232$$

$$\text{Synthetic Hct}_{\text{ShMOLLI}} = (727.1 \cdot [1/T1_{blood}]) - 0.0675$$

where Hct is hematocrit (0 to 1) and $R1_{blood} = (1/T1_{blood})$ in milliseconds.

Using these curve-fits in the validation cohort, synthetic and conventional ECV were highly correlated ($R^2 = 0.97$; $p < 0.001$, both mapping techniques) with a 2.8% SD of differences and minimal bias on Bland-Altman analysis for fibrosis quantification and a slightly higher SD in difference of 5% in extracellular expansion due to amyloidosis (**Figure 2**). Synthetic and conventional ECV correlated equally with clinical markers of disease severity (Online Table S1).

TEST-RETEST VARIABILITY. Bland-Altman comparison of laboratory Hct versus synthetic Hct in the validation cohort revealed a variability of 14%, $R^2 = 0.44$. To understand the sources of variability attributable to laboratory Hct and synthetic Hct (i.e., $T1_{blood}$), test/retest was performed. Test/retest variability of laboratory Hct was higher than expected (n = 44, variability 10% with Hct/Hct $R^2 = 0.86$) (Online Figure S1), where test/retest for $T1_{blood}$ (and by inference, synthetic Hct) in healthy volunteers was low for MOLLI (n = 20, variability 0.02%, $R^2 = 0.95$) (Online Figure S2) and ShMOLLI (n = 20, variability 0.012%, $R^2 = 0.94$). Interobserver reproducibility for $T1_{blood}$ was also excellent (intraclass correlation coefficient 0.994, 95% CI: 0.984 to 0.998).

HISTOLOGY COHORT. The mean histological CVF of the 18 biopsies was 17 ± 8% (range 5% to 40%). Synthetic and conventional ECV both correlated well with collagen volume fraction ($R^2 = 0.61$, $p < 0.001$ vs. $R^2 = 0.69$, $p < 0.001$) (**Figure 3**) and did not differ statistically ($p = 0.70$).

OUTCOME COHORT. Baseline characteristics are presented in **Table 3**. The U.K. derivation resulted in a 2% bias in synthetic ECV; therefore, a local synthetic Hct calibration was obtained (Online Figures S3, S4, and S6). In the outcome cohort, conventional and synthetic ECV had similar ranges (16.6% to 47.8% and 16.2% to 50.9%, respectively) with excellent correlation ($R^2 = 0.82$, $p < 0.001$) (Online Figure S5) and no significant bias. Over a median of 1.7 years

FIGURE 1 Derivation Cohort: Correlation $R1_{blood}$ Versus Hct (MOLLI and ShMOLLI)

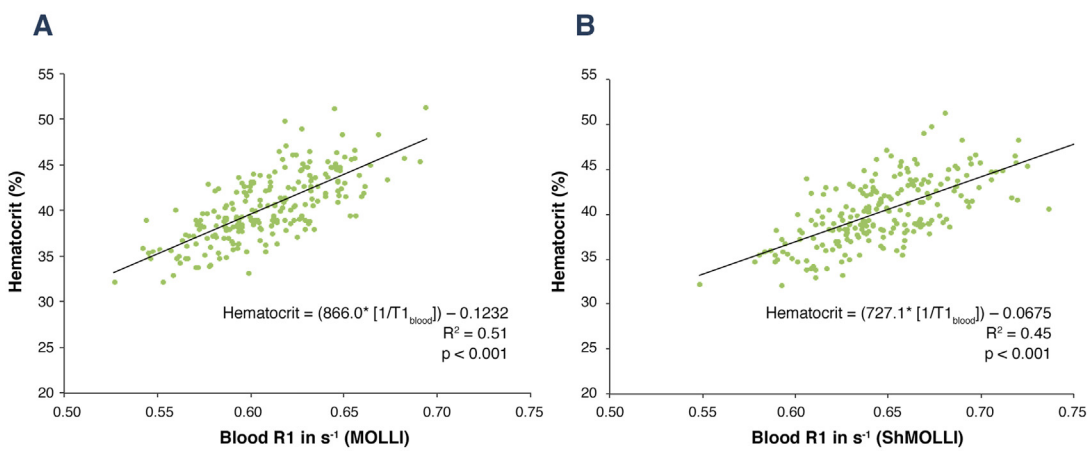

The proof-of-concept cohort was divided randomly into a derivation (n = 214) and a validation (n = 213) cohorts. The regression line between hematocrit and pre-contrast $R1_{blood}$ was linear with $R^2 = 0.51$, $p < 0.001$, and $R^2 = 0.45$, $p < 0.001$, for MOLLI **(A)** and ShMOLLI **(B)** with regression equations as given in the graphs. Hct = hematocrit; MOLLI = MOdified Look-Locker Inversion recovery; ShMOLLI = Shortened MOdified Look-Locker Inversion recovery.

FIGURE 2 Validation Cohort: Conventional Versus Synthetic ECV

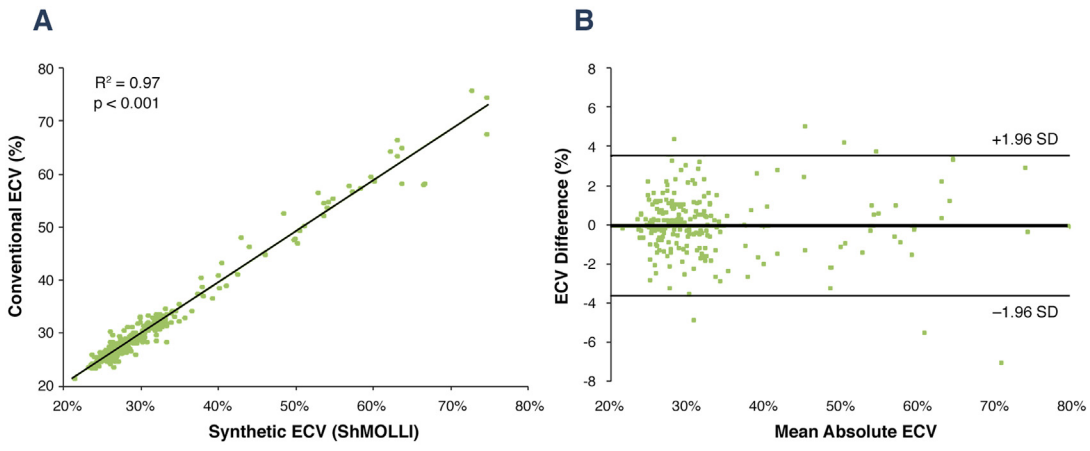

Using these curve-fits in the validation cohort, synthetic and conventional extracellular volume fraction (ECV) were highly correlated ($R^2 = 0.97$; $p < 0.001$, both mapping techniques) with a 2.8% SD of differences and minimal bias on Bland-Altman analysis for fibrosis quantification and a slightly higher SD in difference of 5% in extracellular expansion due to amyloidosis.

(interquartile range: 1.0 to 2.4 years), there were 55 HHF events and 74 deaths after the baseline CMR scan among 111 individuals experiencing adverse events in the n = 1,172 cohort (18 individuals experiencing HHF subsequently died). Synthetic and conventional ECV were associated with adverse events with a graded response, where higher ECV was associated with higher event rates (**Figure 4**). Conventional and synthetic ECV were comparable to the ejection fraction in their univariable association with HHF, but ECV (conventional and synthetic) was better than the ejection fraction for mortality (**Table 4**).

AUTOMATED INLINE SYNTHETIC ECV COHORT: REAL-WORLD APPLICATION. A module was created to generate automatic synthetic ECV maps inline ("on-the-fly") as post-contrast T1 maps are acquired (**Figure 5**, Online Video 1). The additional processing time is <1 s per slice for finding paired pre-contrast T1 mapping data, performing image coregistration, and generating the blood mask and synthetic ECV map. The user is able to analyze images immediately by drawing regions of interest on the scanner console, where pixel values represent percentage ECV.

DISCUSSION

CMR extracellular volume quantification is a promising imaging biomarker (33-35), but development and clinical uptake have been slowed by the necessity of venous blood sampling, analysis, and then offline calculation. We implemented a simpler, synthetic ECV measured using hematocrit estimated from pre-contrast blood T1. Synthetic ECV performed well: it is highly correlated to conventional ECV, and has a similar relationship to the histologic gold standard CVF, other cardiac parameters, and predicts outcome similarly, even at a different center. The implementation here as an inline tool on a clinical CMR scanner would be an aid to clinical

FIGURE 3 Histology Cohort: Conventional ECV and Synthetic ECV Versus CVF

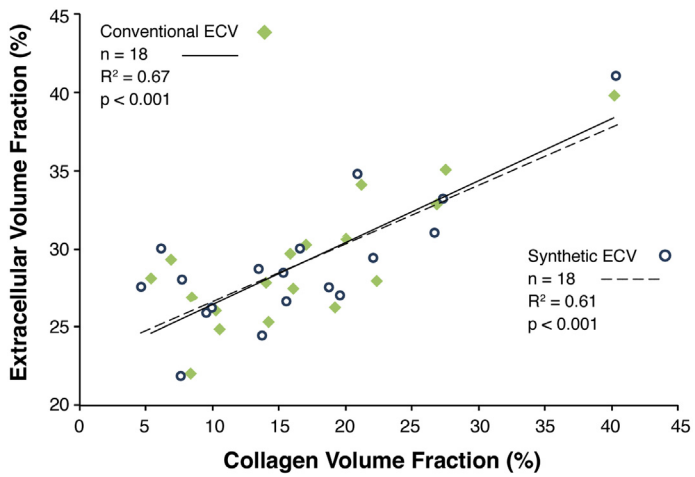

The mean histological collagen volume fraction (CVF) of the 18 biopsies was 17 ± 8% (range 5% to 40%). The correlation with histology for synthetic extracellular volume fraction (ECV) was slightly lower than the conventional ECV ($R^2 = 0.61$, $p < 0.0.01$ vs. $R^2 = 0.69$, $p < 0.001$) but did not differ statistically ($p = 0.70$).

JACC: CARDIOVASCULAR IMAGING, VOL. 9, NO. 1, 2016
JANUARY 2016:54–63

FIGURE 4 Outcome Cohort: Kaplan-Meier Plot (Death and HHF) for ECV

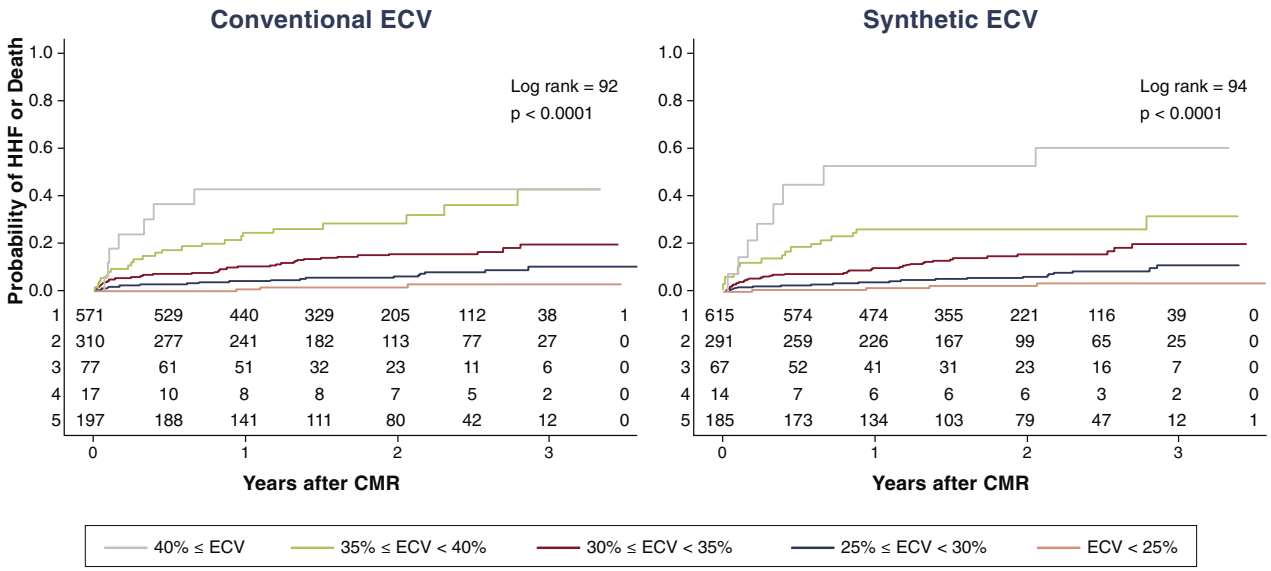

Among 1,172 individuals, both conventional and synthetic myocardial extracellular volume fraction (ECV) were significantly associated with increased risks of hospitalization for heart failure (HHF) or death (n = 111) following cardiac magnetic resonance (CMR) scanning.

workflow, providing automated immediate point-of-care results.

The technique arose out of need and the observation that pre-contrast blood T1 is considerably determined by hematocrit (pre-contrast blood T1 increases with anemia). Indeed, the linear relationship between Hct and $R1_{blood}$ ($1/T1_{blood}$) has been abundantly described (7,14–20), and therefore, $R1_{blood}$ was used for curve fitting. Beyond mathematical derivation, we describe $1/T1_{blood}$ because it is more intuitive for the CMR clinicians and easier to sell to the CMR community. This is analogous to the T2* field that uses T2* rather than the R2*. Although the correlation of peripheral Hct and ventricular cavity pre-contrast $R1_{blood}$ is only moderate (other influences are discussed in the following text), synthetic ECV performance is good, which we believe is in part due to considerable error in standard laboratory Hct when taken as a routine clinical test, and also because the ECV has other dependencies that make it robust (6,9,10,36). It may be that an overlooked weakness has been the variability of Hct measurement (37). Here, the correlation of 2 Hct samples on the same day to a clinical service (located in a different building so with potential settling and re-suspension of red cells during transport) was only a R^2 of 0.86—potentially a greater source of inaccuracy than the differences contested between T1 mapping approaches (30,38).

ECV is gaining recognition as a potentially key biomarker of ECM expansion and has been called "noninvasive" or "virtual biopsy" (39). The near-exponential increase of evidence for the role of T1 mapping and ECV quantification for myocardial tissue characterization calls for the routine clinical use beyond late gadolinium enhancement (Novel Markers of Prognosis in Hypertrophic Cardiomyopathy; [HCMR Study]; NCT01915615). Separate analysis of pre- and post-contrast images is cumbersome. Although implementation of automated ECV map tools is simplifying this (40), Hct measure is

TABLE 4 Conventional and Synthetic ECV and LVEF Were Comparable in Their Univariable Association With HHF, Mortality, or Combined

Outcome	Univariable Cox Regression Model Covariate	Hazard Ratio (95% CI)	Chi-Square	p Value
HHF (n = 55)	Conventional ECV (5% increase)	2.41 (1.93–3.02)	59.6	<0.001
	Synthetic ECV (5% increase)	2.30 (1.87–2.81)	64.5	<0.001
	LVEF (5% decrease)	1.33 (1.23–1.43)	54.3	<0.001
Death (n = 74)	Conventional ECV (5% increase)	2.13 (1.74–2.61)	53.4	<0.001
	Synthetic ECV (5% increase)	1.90 (1.55–2.31)	39.8	<0.001
	LVEF (5% decrease)	1.21 (1.16–1.29)	32.0	<0.001
HHF or death (n = 111)	Conventional ECV (5% increase)	2.25 (1.91–2.64)	96.0	<0.001
	Synthetic ECV (5% increase)	2.06 (1.77–2.40)	89.2	<0.001
	LVEF (5% decrease)	1.26 (1.19–1.33)	71.7	<0.001

ECV = extracellular volume fraction; HHF = hospitalization for heart failure; LVEF = left ventricular ejection fraction.

FIGURE 5 Automatic Synthetic ECV Tool: ECV Mapping "on-the-Fly"

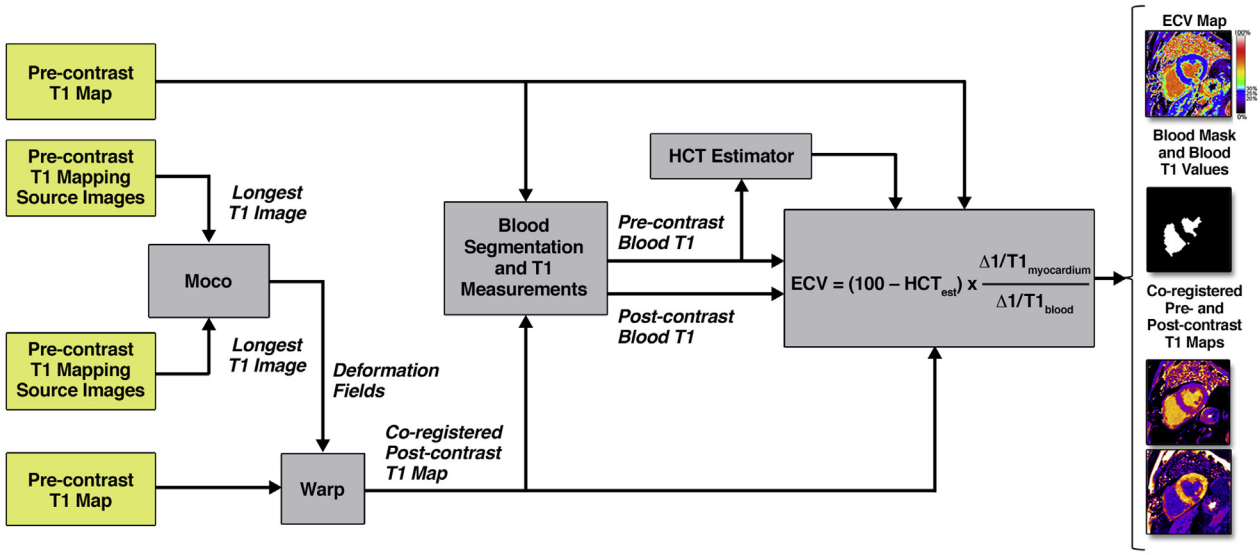

An automated inline synthetic extracellular volume fraction (ECV) tool was implemented as an investigational prototype to produce a fast and fully automated approach for generating pixel-wise synthetic ECV maps (Online Video 1).

burdensome in busy departments, is a source of user error, and introduces reporting delay. An inline synthetic ECV tool would reduce the barriers to clinical use of ECV and potentially increase quality as review is immediate.

STUDY LIMITATIONS. Although this study was not a multicenter study, following validation and derivation in a single center, we then tested outcome in a separate center. The T1 mapping methods varied across parts of experiments (in line with rapid developments within the T1 mapping field), and further comparisons are required. As for any other non-contrast mapping parameter, synthetic Hct requires local calibration, unless T1 mapping sequence, CMR scanner, and Hct machine are identical. Other sources that affect the relaxation rate of blood such as flow, oxygen content, body temperature, and contributions from other biological variables need further investigation (e.g., red cell shape and size, other macromolecules, and even added substances, e.g., intravenous iron or other paramagnetic substances) (7,14,17,18,41-43). In iron overload, particularly in thalassemia patients, the R1/Hct relationship breaks down (unpublished data), which may to be due to iron-chelator complexes. Finally, there are additional influences on measured $T1_{blood}$ (e.g., residual heart rate dependence with some sequences, where measured $T1_{blood}$ decreases with increasing heart rate). The range of diseases studied was not exhaustive, and extreme patients (e.g., very anemic) are not well represented. Variability of repeat synthetic ECV was not tested due to the requirement to use gadolinium contrast to assess this, but variability of $T1_{blood}$, and thereby synthetic Hct, was low across repeated scans, making it a suitable tool for clinical trials (44). The synthetic ECV approach highlights Hct measurement issues that may be easily solved without resorting to new approaches, improving the conventional ECV method.

CONCLUSIONS

The CMR biomarker ECV is promising as a measure of the myocardial interstitial space and can be simplified and automated by using a synthetic Hct. Synthetic ECV is validated in health and disease, against histology, across centers, and predicts outcome as well as the conventional ECV. Automated synthetic ECV measures can be implemented inline on the CMR scanner with test performances approaching that of conventional ECV measurement—a significant workflow improvement bringing ECV closer to routine clinical practice.

REPRINT REQUESTS AND CORRESPONDENCE: Prof James C. Moon, The Heart Hospital Imaging Centre and Barts Heart Centre, St Bartholomew's Hospital, 2nd Floor, King George V Block, London EC1A 7BE, United Kingdom. E-mail: j.moon@ucl.ac.uk.

JACC: CARDIOVASCULAR IMAGING, VOL. 9, NO. 1, 2016
JANUARY 2016:54–63

PERSPECTIVES

COMPETENCY IN MEDICAL KNOWLEDGE: ECV is a promising imaging biomarker, but requires venous blood sampling for analysis and offline calculation. A simpler, synthetic ECV can be measured using hematocrit estimated from the longitudinal relaxation rate of blood. Synthetic ECV is highly correlated to conventional ECV, validated against histology and predicts outcome similarly, even at a different center. Implementation of an automatic inline tool on a clinical CMR scanner can aid clinical workflow, providing immediate point-of-care results.

TRANSLATIONAL OUTLOOK: The synthetic ECV approach highlights hematocrit measurement issues that may be easily solved without resorting to new approaches, improving the conventional ECV method. Synthetic hematocrit requires local calibration, unless T1 mapping sequence, CMR scanner and hematocrit machine are identical. Other sources that affect the relaxation rate of blood such as flow, oxygen content, body temperature, and contributions from other biological variables need further investigation.

REFERENCES

1. Weber KT, Brilla CG. Pathological hypertrophy and cardiac interstitium. Fibrosis and renin-angiotensin-aldosterone system. Circulation 1991;83:1849–65.

2. van Hoeven KH, Factor SM. A comparison of the pathological spectrum of hypertensive, diabetic, and hypertensive-diabetic heart disease. Circulation 1990;82:848–55.

3. Rossi MA. Pathologic fibrosis and connective tissue matrix in left ventricular hypertrophy due to chronic arterial hypertension in humans. J Hypertens 1998;16:1031–41.

4. Beltrami CA, Finato N, Rocco M, et al. Structural basis of end-stage failure in ischemic cardiomyopathy in humans. Circulation 1994;89:151–63.

5. Mewton N, Liu CY, Croisille P, Bluemke D, Lima JA. Assessment of myocardial fibrosis with cardiovascular magnetic resonance. J Am Coll Cardiol 2011;57:891–903.

6. Ugander M, Oki AJ, Hsu LY, et al. Extracellular volume imaging by magnetic resonance imaging provides insights into overt and sub-clinical myocardial pathology. Eur Heart J 2012;33:1268–78.

7. Piechnik SK, Ferreira VM, Lewandowski AJ, et al. Normal variation of magnetic resonance T1 relaxation times in the human population at 1.5 T using ShMOLLI. J Cardiovasc Magn Reson 2013;15:13.

8. Moon JC, Messroghli DR, Kellman P, et al. Myocardial T1 mapping and extracellular volume quantification: a Society for Cardiovascular Magnetic Resonance (SCMR) and CMR Working Group of the European Society of Cardiology consensus statement. J Cardiovasc Magn Reson 2013;15:92.

9. Wong TC, Piehler K, Meier CG, et al. Association between extracellular matrix expansion quantified by cardiovascular magnetic resonance and short-term mortality. Circulation 2012;126:1206–16.

10. Wong TC, Piehler KM, Kang IA, et al. Myocardial extracellular volume fraction quantified by cardiovascular magnetic resonance is increased in diabetes and associated with mortality and incident heart failure admission. Eur Heart J 2014;35:657–64.

11. Messroghli DR, Radjenovic A, Kozerke S, Higgins DM, Sivananthan MU, Ridgway JP. Modified Look-Locker inversion recovery (MOLLI) for high-resolution T1 mapping of the heart. Magn Reson Med 2004;52:141–6.

12. Piechnik SK, Ferreira VM, Dall'Armellina E, et al. Shortened Modified Look-Locker Inversion recovery (ShMOLLI) for clinical myocardial T1-mapping at 1.5 and 3 T within a 9 heartbeat breathhold. J Cardiovasc Magn Reson 2010;12:69.

13. Kellman P, Hansen MS. T1-mapping in the heart: accuracy and precision. J Cardiovasc Magn Reson 2014;16:2.

14. Fullerton GD, Potter JL, Dornbluth NC. NMR relaxation of protons in tissues and other macromolecular water solutions. Magn Reson Imaging 1982;1:209–26.

15. Braunschweiger PG, Schiffer L, Furmanski P. The measurement of extracellular water volumes in tissues by gadolinium modification of 1H-NMR spin lattice (T1) relaxation. Magn Reson Imaging 1986;4:285–91.

16. Martin MA, Tatton WG, Lemaire C, Armstrong RL. Determination of extracellular/intracellular fluid ratios from magnetic resonance images: accuracy, feasibility, and implementation. Magn Reson Med 1990;15:58–69.

17. Lu H, Clingman C, Golay X, van Zijl PC. Determining the longitudinal relaxation time (T1) of blood at 3.0 Tesla. Magn Reson Med 2004;52:679–82.

18. Shimada K, Nagasaka T, Shidahara M, Machida Y, Tamura H. In vivo measurement of longitudinal relaxation time of human blood by inversion-recovery fast gradient-echo MR imaging at 3T. Magn Reson Med Sci 2012;11:265–71.

19. Li W, Grgac K, Huang A, Yadav N, Qin Q, van Zijl PC. Quantitative theory for the longitudinal relaxation time of blood water. Magn Reson Med 2015 Aug 18 [E-pub ahead of print].

20. Spees WM, Yablonskiy DA, Oswood MC, Ackerman JJ. Water proton MR properties of human blood at 1.5 Tesla: magnetic susceptibility, T(1), T(2), T*(2), and non-Lorentzian signal behavior. Magn Reson Med 2001;45:533–42.

21. Elliott P, Andersson B, Arbustini E, et al. Classification of the cardiomyopathies: a position statement from the European Society Of Cardiology Working Group on Myocardial and Pericardial Diseases. Eur Heart J 2008;29:270–6.

22. Perugini E, Guidalotti PL, Salvi F, et al. Noninvasive etiologic diagnosis of cardiac amyloidosis using 99mTc-3,3-diphosphono-1,2-propanodicarboxylic acid scintigraphy. J Am Coll Cardiol 2005;46:1076–84.

23. Fontana M, Banypersad SM, Treibel TA, et al. Native T1 mapping in transthyretin amyloidosis. J Am Coll Cardiol Img 2014;7:157–65.

24. White SK, Sado DM, Fontana M, et al. T1 mapping for myocardial extracellular volume measurement by CMR: bolus only versus primed infusion technique. J Am Coll Cardiol Img 2013;6:955–62.

25. Schelbert EB, Piehler KM, Zareba KM, et al. Myocardial fibrosis quantified by extracellular volume is associated with subsequent hospitalization for heart failure, death, or both across the spectrum of ejection fraction and heart failure stage. J Am Heart Assoc 2015;4:e002613.

26. Kellman P, Wilson JR, Xue H, Ugander M, Arai AE. Extracellular volume fraction mapping in the myocardium, part 1: evaluation of an automated method. J Cardiovasc Magn Reson 2012;14:63.

27. Kellman P, Wilson JR, Xue H, et al. Extracellular volume fraction mapping in the myocardium, part 2: initial clinical experience. J Cardiovasc Magn Reson 2012;14:64.

28. Kramer CM, Barkhausen J, Flamm SD, Kim RJ, Nagel E. Standardized cardiovascular magnetic resonance imaging (CMR) protocols, society for cardiovascular magnetic resonance: board of

trustees task force on standardized protocols. J Cardiovasc Magn Reson 2008;10:35.

29. White SK, Treibel TA, Moon JC. Reply: effects of blood T1 on extracellular volume calculation. J Am Coll Cardiol Img 2014;7:849–50.

30. Kellman P, Arai AE, Xue H. T1 and extracellular volume mapping in the heart: estimation of error maps and the influence of noise on precision. J Cardiovasc Magn Reson 2013;15:56.

31. Xue H, Shah S, Greiser A, et al. Motion correction for myocardial T1 mapping using image registration with synthetic image estimation. Magn Reson Med 2012;67:1644–55.

32. Hill VL, Simpson VZ, Higgins JM, et al. Evaluation of the performance of the Sysmex XT-2000i Hematology Analyzer with whole bloods stored at room temperature. Lab Med 2009;40:709–18.

33. Schelbert EB, Fonarow GC, Bonow RO, Butler J, Gheorghiade M. Therapeutic targets in heart failure: refocusing on the myocardial interstitium. J Am Coll Cardiol 2014;63:2188–98.

34. Sado DM, Flett AS, Banypersad SM, et al. Cardiovascular magnetic resonance measurement of myocardial extracellular volume in health and disease. Heart 2012;98:1436–41.

35. Liu CY, Liu YC, Wu C, et al. Evaluation of age-related interstitial myocardial fibrosis with cardiac magnetic resonance contrast-enhanced T1 mapping: MESA (Multi-Ethnic Study of Atherosclerosis). J Am Coll Cardiol 2013;62:1280–7.

36. Banypersad SM, Fontana M, Maestrini V, et al. T1 mapping and survival in systemic light-chain amyloidosis. Eur Heart J 2015;36:244–51.

37. Thirup P. Haematocrit: within-subject and seasonal variation. Sports Med 2003;33:231–43.

38. Roujol S, Weingartner S, Foppa M, et al. Accuracy, precision, and reproducibility of four T1 mapping sequences: a head-to-head comparison of MOLLI, ShMOLLI, SASHA, and SAPPHIRE. Radiology 2014;272:683–9.

39. Kramer CM, Chandrashekhar Y, Narula J. T1 mapping by CMR in cardiomyopathy: a noninvasive myocardial biopsy? J Am Coll Cardiol Img 2013;6:532–4.

40. Spottiswoode BS, Ugander M, Kellman P. Automated inline extracellular volume (ECV) mapping (abstr). J Cardiovasc Magn Reson 2015;17 Suppl 1:W6.

41. Yilmaz A, Bucciolini M, Longo G, Franciolini F, Ciraolo L, Renzi R. Determination of dependence of spin-lattice relaxation rate in serum upon concentration of added iron by magnetic resonance imaging. Clin Phys Physiol Meas 1990;11:343–9.

42. Wright GA, Hu BS, Macovski A. 1991 I.I. Rabi Award. Estimating oxygen saturation of blood in vivo with MR imaging at 1.5 T. J Magn Reson Imaging 1991;1:275–83.

43. Silvennoinen MJ, Kettunen MI, Kauppinen RA. Effects of hematocrit and oxygen saturation level on blood spin-lattice relaxation. Magn Reson Med 2003;49:568–71.

44. Liu S, Han J, Nacif MS, et al. Diffuse myocardial fibrosis evaluation using cardiac magnetic resonance T1 mapping: sample size considerations for clinical trials. J Cardiovasc Magn Reson 2012;14:90.

KEY WORDS collagen, ECV, magnetic resonance imaging, mortality, myocardial fibrosis

APPENDIX For an expanded Methods section, a supplemental video and its legend, and supplemental figures and tables, please see the online version of this article.